AIAA JOURNAL
Vol. 30, No. 8, August 1992

Hypersonic Rarefied Flow About a Delta Wing—Direct Simulation and Comparison with Experiment

M. Cevdet Celenligil*
Vigyan Research Associates, Inc., Hampton, Virginia 23666
and
James N. Moss†
NASA Langley Research Center, Hampton, Virginia 23665

Three-dimensional simulations of hypersonic rarefied flow about a delta wing are performed using the direct simulation Monte Carlo method of Bird, and the results of the computations are compared with recent experimental data obtained in a vacuum wind tunnel at the DLR in Gottingen, Germany. The present study considers Mach 8.89 nitrogen flow for a range of conditions that include Knudsen numbers of 0.016–3.505 for an incidence angle of 30 deg, and angles of incidence of 15–60 deg for a constant Knudsen number of 0.389. The calculations provide details concerning the flowfield structure and surface quantities. Comparisons between the calculations and the available experimental measurements are made for aerodynamic and overall heat transfer coefficients and recovery temperature. The agreement between the measured and calculated data are very good, well within the estimated measurement uncertainty. Comparisons are also made with modified Newtonian and free-molecule theories.

Nomenclature

A = planview area
C_D = drag coefficient
C_H = total heat transfer coefficient
C_L = lift coefficient
C_m = pitching moment coefficient (with respect to the body apex)
D = drag force
d = diameter
Kn = Knudsen number
L = lift force
l = reference length
M = Mach number
p = pressure
$\dot{q}$ = heat transfer rate
R = radius
Re = Reynolds number
T = temperature
T_{int} = internal temperature
T_{ov} = overall temperature
T_r = recovery temperature
T_{tr} = translational temperature
T_w = wall temperature
V = speed
x,y,z = Cartesian coordinates
α = incidence angle of upper surface, positive leeward
η = distance along the stagnation streamline (measured from the body)
ρ = density

Subscripts
ref = reference
∞ = freestream
o = stagnation conditions

Introduction

WITH the demand for improved maneuverability, interest in the design of vehicles of higher aerodynamic coefficients remain high. The use of aerodynamic forces to tailor an orbit or trajectory of a space vehicle can be quite beneficial.[1] For aerocapture and orbital transfer applications, aerodynamic drag is the key factor; whereas for synergetic plane change applications, high lift-to-drag ratio L/D becomes important. A recent application where high L/D is the primary concern has been described by Randolph and McRonald[2] for achieving spacecraft trajectory modification by passing through a planetary atmosphere. Here a conventional gravity assist trajectory can be greatly enhanced by an aerodynamic assist using the vehicles' lift vector to obtain virtually any amount of angular deflection of the trajectory as the vehicle passes through the atmosphere. Design of spacecraft with high aerodynamic coefficiencies will benefit from extended knowledge of this aerothermodynamic behavior in the transitional

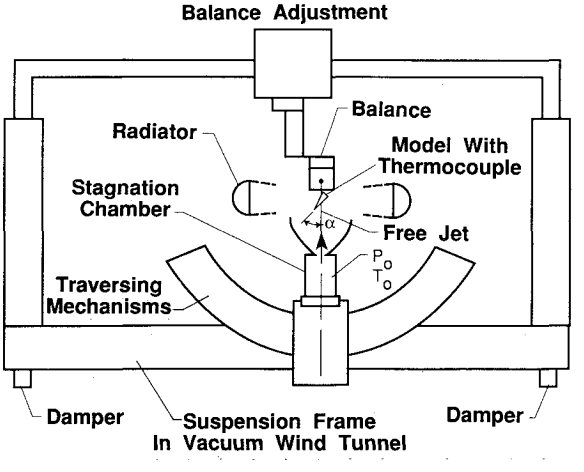

Fig. 1 Experimental setup.

Presented as Paper 91-1315 at the AIAA 26th Thermophysics Conference, Honolulu, HI, June 24–26, 1991; received June 28, 1991; revision received Nov. 27, 1991; accepted for publication Dec. 11, 1991.

*Research Engineer; currently Associate Professor, Aeronautical Engineering Department, Middle East Technical Univ., Ankara 06531, Turkey. Member AIAA.

†Research Engineer, Aerothermodynamics Branch, Space Systems Division. Fellow AIAA.

flow regime; that is, the flow regime between continuum and free-molecular flow.

Today, capability exists for simulating rarefied flows about three-dimensional configurations using either computational or experimental tools. The computational capability is of more recent origin, but has evolved rapidly to the point where it is now being applied to full-scale, three-dimensional flight simulations[3,4] that include chemical reactions. In general, the existing experimental capability is limited to low-enthalpy facilities where small to very small models are used. The present study is focused on applying a three-dimensional direct simulation Monte Carlo (DSMC) computer code to the problem of numerically simulating the nitrogen flow about a highly swept delta-wing model that is 4.86 mm in length and comparing the results with recent experimental measurements.[5] Admittedly, the flow conditions, similar to those obtained in nearly all ground-based experimental facilities, are far from those experienced in flight. Nevertheless, the current flow problem has several distinct physical features and simulating such flows is an important aspect of ongoing code-validation efforts. The experimental data include two-component forces and overall heat transfer rate information. The range of conditions considered in the present study are such that most of the transitional flow regime is covered ($0.016 \leq Kn_\infty \leq 3.505$), where Kn_∞ is the freestream Knudsen number. Also, an angle-of-incidence α variation is considered for $Kn_\infty = 0.389$. This study represents a continuation of recent efforts[6,7] to analyze and compare the DSMC results with wind-tunnel data obtained for a highly swept delta-wing configuration at angle of incidence. Previous calculations were made for one set of test conditions ($Kn_\infty = 0.016$ and $M_\infty = 20.2$), where M_∞ is the freestream Mach number and a body length of 100 mm. Comparisons with the experimental data of Allegre et al.[8,9] showed reasonably good agreement for the leeside density contours. However, discrepancies exist between the experimental and calculated results for the drag and lift coefficients. These differences may be caused by inadequately defined freestream conditions, since the experiments were performed in a flow environment where gradients exist[9] in both the radial and axial directions (open test section with flow from a conical nozzle followed by a cylindrical extension) and the numerical simulation was made assuming a uniform freestream condition corresponding to undisturbed freestream conditions at the model apex. The sensitivity of the numerical simulations to modeled radial density variations (not the actual nozzle flow which included axial and angular variations) have been investigated by Rault[10] for the same delta wing. Rault's findings[10] suggest that the flow nonuniformity is indeed one of the likely causes for the differences between the measured and calculated results.

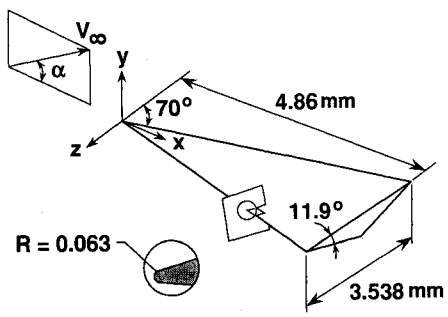

Fig. 2 Schematic of the delta wing (dimensions in milimeters).

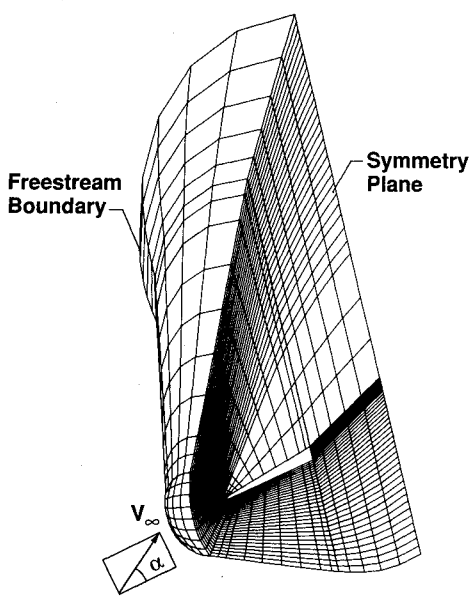

Fig. 3 Perspective view of three-dimensional computational grid.

The present study focuses on a much smaller version (4.86-% scale) of the same delta wing where the flow is produced by a freejet expansion. Again, gradients exist in the flow; however, the model is quite small and the experimental data reduction procedures[5] attempted to minimize the effects of the departure from parallel flow on the measured coefficients by using undisturbed freestream properties at the model 2/3-chord location.

Experimental Facility

The experimental measurements were performed by Legge[5] using the V3G vacuum wind tunnel at the DLR in Gottingen, Germany. The experimental arrangement for the force and heat transfer measurements on the delta wing is shown schematically in Fig. 1. The flow is produced by a freejet expansion emanating from a stagnation chamber with an effective orifice diameter of 3.802 mm. (The geometric diameter is 3.96 mm.) The data presented in Ref. 5 were obtained with the stagnation chamber in the vertical position as shown in Fig. 1, and the model was oriented to achieve the desired angle of incidence. With this arrangement, the model provided a more effective shield for the suspension. The distance between the orifice and delta wing was fixed at 40 mm (10.52 orifice diameters). The 40-mm distance is that between the orifice and the 2/3-chord location on the centerline of the upper (flat) surface of the model. As for the Mach disk location, it was 25–30 cm from the orifice for nitrogen flow.

A recently developed two-component electromagnetic balance[11] was used to measure the lift and drag forces. The freestream flow quantities at the 2/3-chord location are used to nondimensionalize the force measurements and overall heat transfer rate. More extensive details of the test facility and experimental methods are given in Refs. 5 and 11. The net measurement uncertainty in the C_L, C_D, and C_H values (due to effects of suspension, flow shield, instrumentation, inaccuracies of the model, gradients in the radial flowfield, etc.) is estimated[5] to be $\pm$ 8%.

Computational Methods

Over the past 25 years, direct simulation techniques have evolved as powerful physical models for the simulation of rarefied flows in which the mean free path of the gas molecules is comparable with the body size. In the present study, the DSMC method of Bird[12–14] is used to simulate a rarefied flow about a delta wing. The DSMC method simulates rarefied flows by keeping track of the motion and internal energies of thousands of representative molecules in the flowfield. The molecular motion is computed for small time increments during which the molecular motion and collision processes are uncoupled. In this study, the molecular collisions are modeled using the variable hard sphere (VHS) molecular model[13] which treats the molecules as hard spheres as far

Table 1 Freestream conditions and computational results for delta wing[a]

Kn_∞	$\rho_\infty \times 10^5$, kg/m^3	Re_∞	C_D	C_L	C_m	C_H	T_r, K
Free molecule	—	—	1.507	0.454	0.798	0.089	341
3.505	0.172	3.1	1.478	0.457	0.787	0.083	339
1.168	0.517	9.2	1.443	0.466	0.774	0.079	337
0.389	1.550	27.6	1.296	0.469	0.714	0.057	330
0.135	4.471	79.5	1.051	0.467	0.611	0.027	315
0.045	13.412	238.4	0.785	0.460	0.517	0.002	295
0.016	38.033	676.1	0.613	0.456	0.462	−0.006	283
Modified Newtonian	—	—	0.325	0.460	0.376	—	—

[a]For all cases: $V_\infty = 756$ m/s, $M_\infty = 8.89$, $T_\infty = 17.4$ K, $T_w = T_o = 293$ K, $\alpha = 30$ deg, and $A = 8.6$ mm^2.

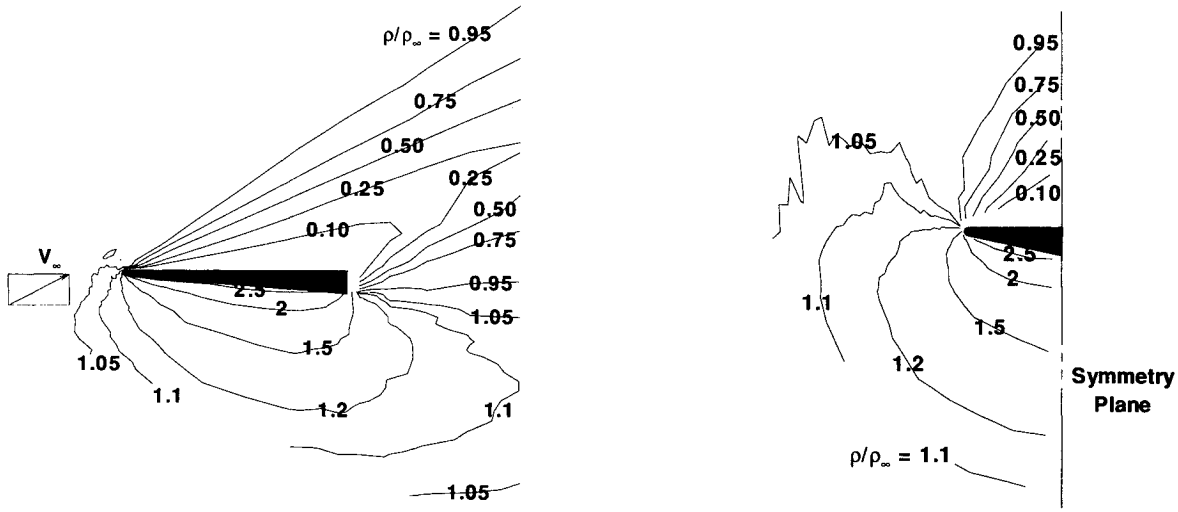

a) Near the symmetry plane

b) Cross section at 80% chord

Fig. 4 Flowfield density contours ($Kn_\infty = 0.389$).

as the scattering angle distribution is concerned, but the collision cross section depends on the relative speed of colliding molecules. Energy exchange between kinetic and internal modes is controlled by the Larsen-Borgnakke statistical model. The three-dimensional computational domain is divided into a network of deformed hexahedral (six-faced) cells, and each cell is further divided into six tetrahedral subcells. The collision partners are selected probabilistically from molecules in the same tetrahedral subcells.

Geometry and Boundary Conditions

This study concentrates on the three-dimensional hypersonic rarefied flow about a delta wing, a sketch of which is shown in Fig. 2. As shown in this figure, the top of the wing is flat, the bottom is V-shaped, and the edges are rounded with a constant radius, $R = 0.0632$ mm. The shape of the nose from the side view is elliptical although it appears sharp from the top view. The origin of the coordinate system is located at the tip of the nose, and the x axis is parallel to the top surface and is normal to the base plane. The angle of incidence is measured with respect to the top surface of the model. The vertical midplane (at $z = 0$) is a plane of symmetry, thus computations have been done on half of the geometry. Figure 3 shows a perspective view for the three-dimensional computational grid used in this study. The body-fitted grid has $4 \times 8 \times 30$ cells around the body apex, $14 \times 16 \times 30$ cells in the midsection, and $4 \times 8 \times 5$ cells at the aft end, i.e., a total of 7840 cells. In the geometrical treatment of the body nose and side edges, six cells are placed in the circumferential direction. The cell size (in the direction normal to the body apex) is 0.03 mm (for the $Kn_\infty = 0.389$ calculations) which is quite conservative due to the fact that the flow is highly rarefied near the tip. This particular test case has also been computed with half of the cell size in the whole domain, and the change in C_D and C_L was less than 2%, and the change in C_H was less than 4%.

The upstream freestream conditions used in the DSMC simulation are uniform and correspond to the nominal conditions specified for the experiments. These nominal conditions correspond to the undisturbed flow quantities at the 2/3-chord location. Table 1 presents the freestream conditions and selected results (for $\alpha = 30$ deg) for the Kn_∞ range considered. Also included are the free-molecule and modified Newtonian results. The freestream mean free path was evaluated using the variable hard sphere (VHS) collision model[13] with $T_{\text{ref}} = 300$ K, $d_{\text{ref}} = 4.07 \times 10^{-10}$ m, and the temperature exponent of the viscosity coefficient of 0.75. The overall Knudsen number based on body length is included in Table 1. The body surface is specified to be at a uniform temperature of 293 K. Full thermal accommodation and diffuse reflection are assumed for the gas-surface interaction. Simulations are performed using a nonreacting gas model with one chemical species (N_2) while considering energy exchange between translational and internal (rotational and vibrational) modes. The rotational and vibrational relaxation collision numbers are 5 and 50, respectively.

Computational Results

The computations are performed for a total of 6900 timesteps. A stationary state was reached around 500 timesteps, and after that, samples are taken every other timestep. Hence the time-averaged results presented in this study are based on samples gathered over 3200 timesteps. The $Kn_\infty = 0.389$ case is computed using 150,000 simulated molecules and 41 h of CPU time on a CRAY-2 computer. For the cases considered, the computational time increases with increasing freestream density. However, all runs are performed using the same number

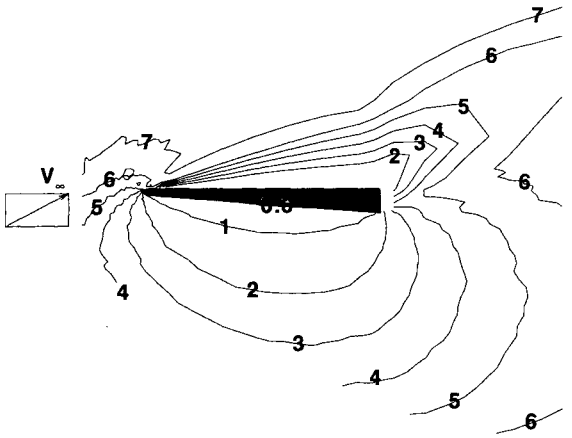

Fig. 5 Mach number contours (near symmetry plane, $Kn_\infty = 0.389$).

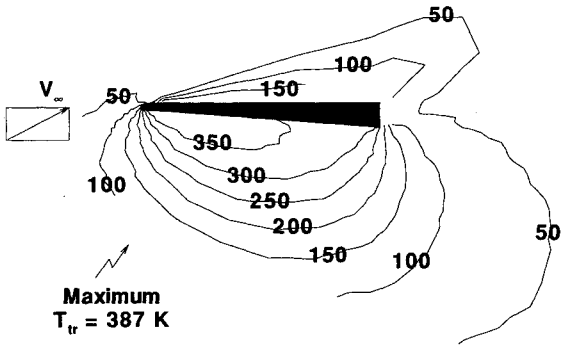

Fig. 6 Flowfield translational temperature contours (near symmetry plane, $Kn_\infty = 0.389$).

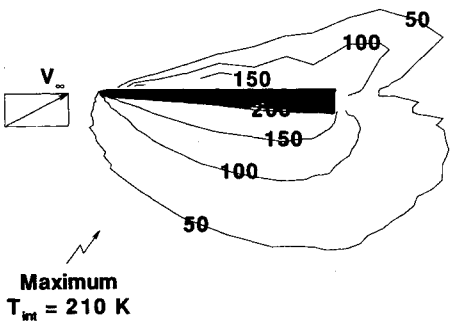

Fig. 7 Flowfield internal temperature contours (near symmetry plane, $Kn_\infty = 0.389$).

of cells and, consequently, the extent of the computational domain (and hence the cells' sizes) is reduced for the less rarefied cases. Also, in order to reduce the computational time for lower Knudsen number runs, less stringent conditions are stipulated such as the cell sizes are allowed to be of the order of the local mean free path rather than one-third of it. Consequently, the run time for the lowest Knudsen number ($Kn_\infty = 0.016$) case (simulated by 120,000 molecules) is only about 3.5 times longer than that for the highest Knudsen number ($Kn_\infty = 3.505$) case (simulated by 85,000 molecules).

Figures 4–7 present some of the flowfield contours. The calculated flowfield results are obtained at the cell centroids and do not extend to the boundaries (one half-cell from the boundaries). Hence, the flowfield contours for the symmetry plane are actually one-half cell from the symmetry plane. The density contours at a cross section located at 80% of the chord length is shown in Fig. 4b.

The flowfield quantities along the stagnation streamline are presented in Fig. 8 which clearly shows the characteristic features of rarefied flows, namely, a significant degree of thermal nonequilibrium, velocity slip, temperature jump, and no distinct shock-wave structure. The stagnation streamline in this figure is an approximate one in that it is generated by a straight line parallel to the freestream velocity vector passing through the point on the surface where the pressure and heat transfer rate are maximum.

Surface pressure and heat transfer rate contours on the windward side are presented in Figs. 9 and 10, respectively. Note that for this problem, the sharp V-shaped bottom edge and the side edges are leading edges, and the high values for pressure and heat transfer rate are due to the leading-edge effects. The surface results are obtained at the centroids of surface elements which are in the form of deformed rectangles. The presented surface results are on the surface, but as with the flowfield contours, the surface contours extend only to within one-half cell of the edges.

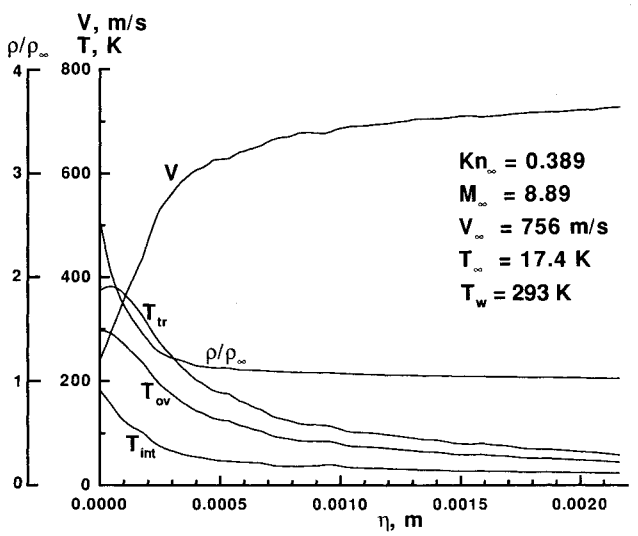

Fig. 8 Flowfield quantities along stagnation streamline.

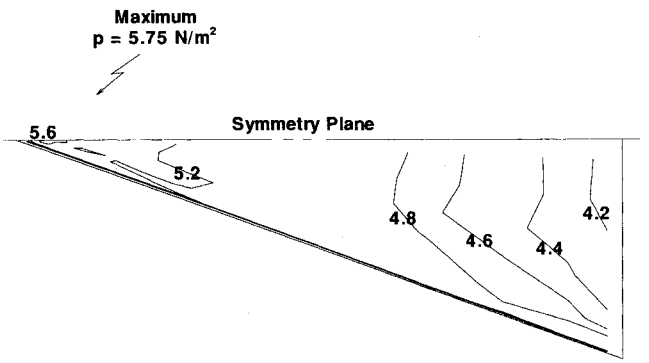

Fig. 9 Surface pressure contours (windward side, $Kn_\infty = 0.389$).

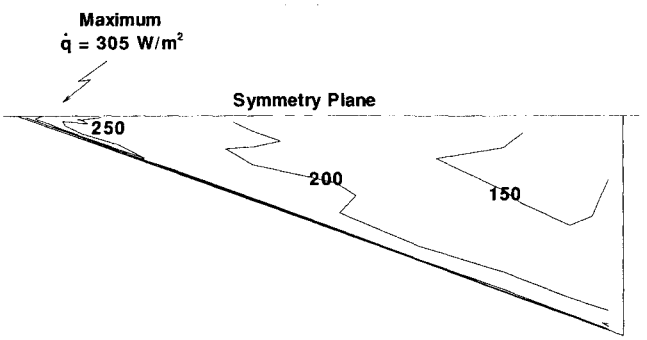

Fig. 10 Surface heat transfer rate contours (windward side, $Kn_\infty = 0.389$).

In this study, the effects of rarefaction have also been investigated. Calculations have been performed for various values of freestream molecular mean free paths by varying the freestream density and keeping the other freestream conditions constant. The results are shown in Fig. 11 for density contours and in Figs. 12 and 13 in terms of aerodynamic and heat transfer coefficients and recovery temperature.

Also, various angle-of-incidence calculations have been performed. Figure 14 shows some of these results. Note that the drag and lift coefficients are normalized with respect to $\frac{1}{2}\rho_\infty V_\infty^2 A$ and the heat transfer coefficient is normalized by $\frac{1}{2}\rho_\infty V_\infty^3 A$, where "$A$" is the planview area of the wing with a value of 8.6 mm^2. The good agreement between the measured and calculated results are evident from the comparisons shown in Figs. 12–14.

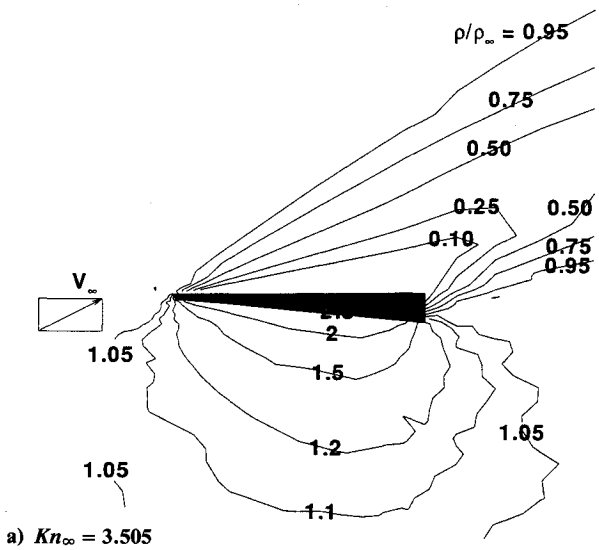

a) $Kn_\infty = 3.505$

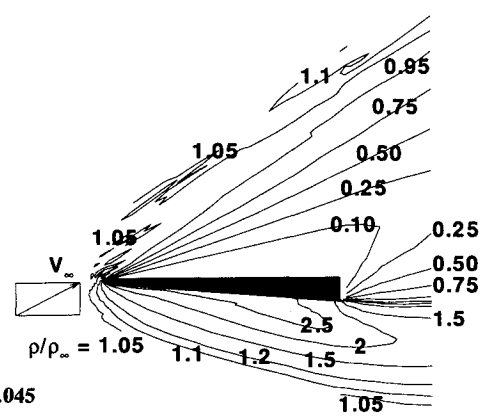

b) $Kn_\infty = 0.045$

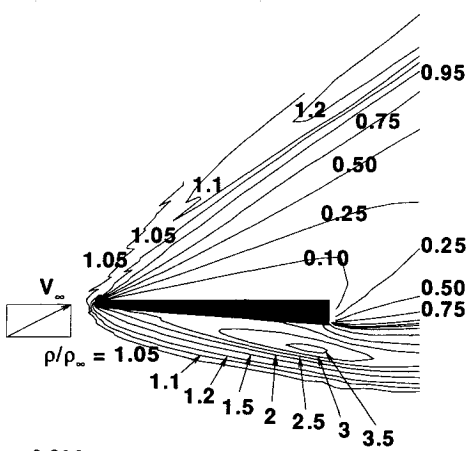

c) $Kn_\infty = 0.016$

Fig. 11 Flowfield density contours (near the symmetry plane).

Discussion

This section will first examine some of the features of the computed flowfield and surface results and then concludes with a discussion of the extent of the agreement between the computed and measured results.

Computational Results

The computed results show some interesting features for the flowfield structure that develops about the delta-wing model considered in the present study. First, the flow is quite rarefied for the range of conditions ($0.016 \leq Kn_\infty \leq 3.5$) considered, and no evidence of separated flow is observed. The extent of the rarefaction is clearly evident from the density contours shown in Figs. 4a and 11a–11c. The maximum density occurs downstream of the tip of the wing rather than at the tip. For the most rarefied case considered (Fig. 11a), the density distribution near the surface and along the symmetry plane is nearly constant. This is the correct behavior as the flow approaches the free-molecule limit. As the Knudsen number is reduced, the maximum density occurs at a location off the body (observed in Ref. 6) rather than on or near the body surface because of the hot wall condition ($T_w/T_o = 1.0$).

For the leeside flow, one finds no evidence of a shock along the symmetry plane for the more rarefied conditions ($Kn_\infty > 0.045$). This is a situation where the density simply increases monotonically from the value adjacent to the top surface to that of the freestream. For Knudsen numbers of 0.045 and smaller, a leeside shock is observed in the symmetry plane and becomes stronger with decreasing Kn_∞. The general features of the leeside flow for $Kn_\infty = 0.016$ are similar to those observed in Refs. 6 and 7 for the same Knudsen number flow (a large model of the same delta wing in Mach 20.2 flow).

The sensitivity of the aerodynamic force coefficients to freestream Knudsen number is demonstrated by the results shown in Table 1 and Fig. 12 for the model at 30-deg angle of incidence. The pitching moment coefficient is normalized with respect to $\frac{1}{2}\rho_\infty V_\infty^2 A l$, where l, the reference length, is 4.86 mm. The figure and table also show the calculated free-molecule and modified Newtonian results. The lift coefficient (Fig. 12a) shows little variation with Knudsen number. This occurs because of the behavior of the pressure and friction forces with increasing rarefaction. Both the pressure and friction coefficients increase with increasing rarefaction, but most of the lift coefficient is due to the positive contribution from the pressure forces on the windward surface and the negative contribution from the skin friction on the same surface. For an angle of incidence of 30 deg, the changes in the two components that contribute to the lift coefficient are comparable in magnitude but opposite in sign; hence the lift coefficient is insensitive to rarefaction effects for a 30-deg angle of incidence.

The impact on the drag coefficient is very different, since the pressure and friction components are additive for most of the windward surface. In fact, the drag coefficient experiences a significant increase with rarefaction and approaches the free-molecule value (within 2% of the free-molecule value at $Kn_\infty = 3.5$).

The calculated thermal response of the model is included in Table 1 and shown in Figs. 13a and 13b for the overall heat transfer coefficient and recovery temperature, respectively. As with the drag coefficient, the heat transfer coefficient approaches the free-molecule results (within 7% of the free-molecule value) for the largest Knudsen number case considered. The model surface temperature for these calculations was constant at 293 K. For the smallest Knudsen number case, the heat transfer coefficient was negative. This is the expected behavior, because it shows that as the freestream density increases (while keeping all other flow parameters constant), the fraction of the energy content of the flow that reaches the

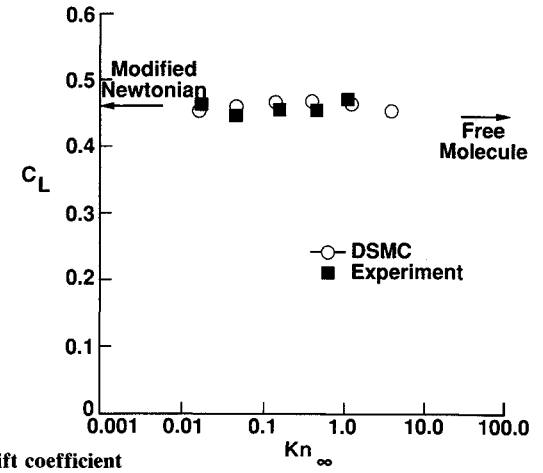

a) Lift coefficient

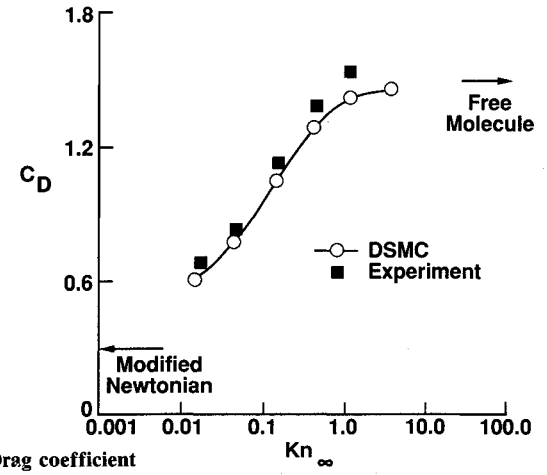

b) Drag coefficient

Fig. 12 Aerodynamic coefficient results for $\alpha = 30$ deg.

surface of the model decreases due to collisions in the shock layer that divert molecules around and away from the model. Thus, for a fixed wall temperature, as the freestream density is increased (Kn_∞ decreased), the overall heat transfer eventually becomes negative (i.e., the recovery temperature becomes less than the wall temperature).

The overall recovery temperature T_r is the wall temperature that produces an overall heat transfer rate of zero for the model. The recovery temperature was determined by performing two or more calculations at each flow condition where the wall temperature was selected to produce both a positive and negative heat transfer coefficient. With this information, a curve is fitted to the calculated data to determine the recovery temperature.

When the wall temperature was altered with respect to the nominal value of $T_w = 293$ K ($T_w/T_o = 1.0$), the impact on the aerodynamic coefficients was significant. For example, for the $Kn_\infty = 0.389$ condition, the recovery temperature was determined by making calculations for wall temperatures of 293, 335, and 380 K. The drag and lift coefficients increased 3.5% and 10.2%, respectively, as the wall temperature was increased from 293 to 380 K. (For $T_w = 335$ K, $C_D = 1.318$ and $C_L = 0.494$. For $T_w = 380$ K, $C_D = 1.341$ and $C_L = 0.518$.)

Finally, the effect of angle of incidence on the aerodynamic and heat transfer coefficients were calculated for a constant Knudsen number condition ($Kn_\infty = 0.389$) and a wall temperature of 293 K. Table 2 presents the results for the coefficients, and Figs. 14a–14c show a comparison of the calculated results with the free-molecule and modified Newtonian values for C_L, C_D, and C_H, respectively. The aerodynamic coefficients follow the free-molecule trends and are relatively close to the free-molecule values. With respect to the free-molecule values, the DSMC results are always greater for lift, less for drag; (trends that one should expect.) For both the drag and heat-transfer coefficients, the DSMC results approach the free-molecule results as the angle of incidence is reduced. Again, this is the anticipated trend, since the flow about the model is actually more rarefied for the lower incidence angles. The increased rarefaction occurs because the effective bluntness of the model is reduced with decreasing angle of incidence, and this produces a lower density flow on the windward surface. This is just another example of the inability of an overall Knudsen number to adequately describe rarefaction effects.

The data shown in Fig. 14a indicate that the lift coefficient will experience a maximum value in the transitional regime provided the angle of incidence is less than about 30 deg. This behavior is very different from that which has been observed for blunt bodies such as the Shuttle Orbiter[4,15] or the Aeroassist Flight Experiment Vehicle[3] where the lift coefficient increases monotonically from the free-molecule value to the continuum value with decreasing rarefaction.

Comparison of Calculated and Measured Results

This section comments briefly on the very good agreement obtained between the experimental measurements of Legge[5] and the present calculations. Figures 12 and 13 show the nature of the agreement for the aerodynamic coefficients (lift and drag) and overall thermal quantities (heat transfer coefficient and recovery temperature) as a function of Kn_∞ for $\alpha = 30$ deg. Figure 14 presents a comparison of the same quantities with the exception of recovery temperature as a function of angle of incidence. It is particularly encouraging to see the good agreement in the heat transfer results (Fig. 13) for the smaller Knudsen number values. For the range of conditions for which comparisons have been presented, the

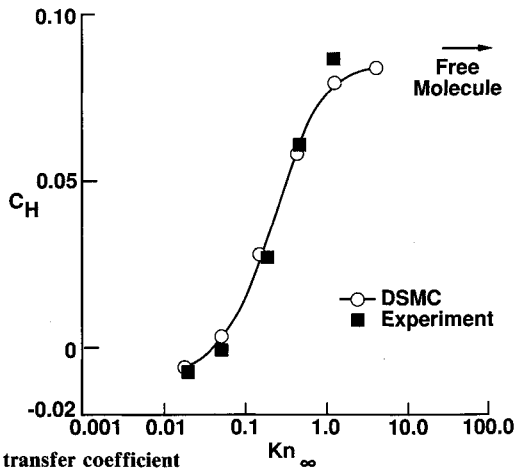

a) Heat transfer coefficient

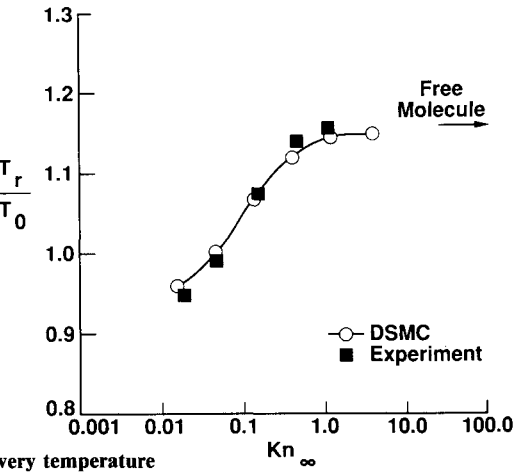

b) Recovery temperature

Fig. 13 Overall thermal quantities for $\alpha = 30$ deg.

Table 2 Computational results as a function of angle of incidence[a]

α, deg	C_D	C_L	L/D	C_m	C_H
15	0.784	0.331	0.423	0.363	0.040
30	1.296	0.469	0.362	0.714	0.057
45	1.785	0.489	0.274	1.076	0.075
60	2.192	0.389	0.177	1.393	0.090

[a]For all cases: $\rho_\infty = 1.55 \times 10^{-5}$ kg/m^3, $V_\infty = 756$ m/s, $M_\infty = 8.89$, $T_\infty = 17.4$ K, $T_w = T_o = 293$ K, $Kn_\infty = 0.389$, $A = 8.6$ mm^2.

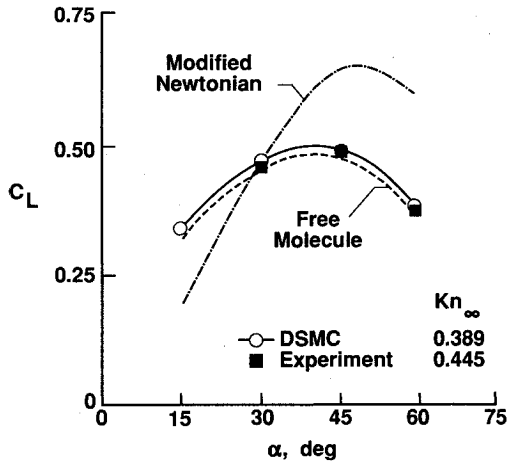

a) Lift coefficient

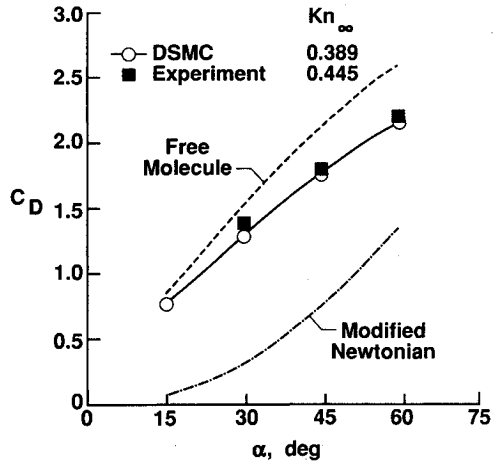

b) Drag coefficient

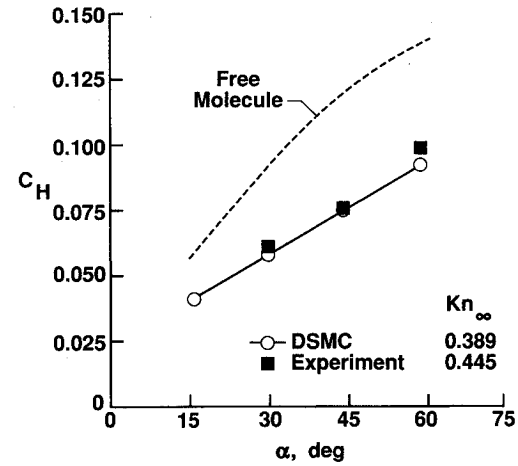

c) Heat transfer coefficient

Fig. 14 Effect of angle of incidence.

calculated data are within the estimated[5] overall experimental uncertainty of ± 8%.

It is appropriate to note that the experiments and calculations were made without prior knowledge of the other's result as part of a hypersonic workshop.[5] What was specified in advance was the flow conditions (i.e., density, temperature, and velocity of the freestream) for $Kn_\infty = 0.389$ which was the primary test condition for the present delta wing at 30-deg incidence. In addition, the range for which additional experimental data would be made available was specified. The experimental data were made available at the workshop as reported in Ref. 5.

Concluding Remarks

In this study, rarefied hypersonic flow about a delta wing has been studied using the direct simulation Monte Carlo method. Calculations are made for freestream Knudsen numbers ranging from 0.016 to 3.5 and for angles of incidence of 15–60 deg. The simulated flow conditions are those corresponding to that produced in a low-density wind tunnel for cold nitrogen flow. The calculations show the flow to the significantly rarefied for the range of conditions considered as evidenced by the aerodynamic coefficients and the flowfield structure. Furthermore, the leeside flow remains attached as evidenced by the surface skin-friction distributions. The agreement between the calculated and measured data are shown to be very good for the aerodynamic and overall heat transfer coefficients and recovery temperatures.

References

[1]Walberg, G. D., "A Survey of Aero-Assisted Orbital Transfer," *Journal of Spacecraft and Rockets,* Vol. 22, No. 1, 1985, pp. 3–18.

[2]Randolph, J. E., and McRonald, A. D., "Solar Probe Mission Status," AAS/GSFC International Symposium on Orbital Mechanics and Mission Design, American Astronomical Society, Paper 89-212, April 24–27, 1989.

[3]Celenligil, M. C., Moss, J. N., and Blanchard, R. C., "Three-Dimensional Rarefied Flow Simulations for the Aeroassist Flight Experiment Vehicle," *AIAA Journal,* Vol. 29, No. 1, 1991, pp. 52–57.

[4]Bird, G. A., "Application of the Direct Simulation Method to the Full Shuttle Geometry," AIAA Paper 90-1692, June 1990.

[5]Legge, H., "Force and Heat Transfer on a Delta Wing in Rarefied Flow," Workshop on Hypersonic Flows for Reentry Problems, Pt. II, Antibes, France, April 1991.

[6]Celenligil, M. C., and Moss, J. N., "Direct Simulation of Hypersonic Rarefied Flow about a Delta Wing," AIAA Paper 90-0143, Jan. 1990.

[7]Celenligil, M. C., and Moss, J. N., "Application of the DSMC Method to Hypersonic Flow about a Delta Wing," 17th International Symposium on Rarefied Gas Dynamics, Aachen, Germany, July 1990.

[8]Allegre, J., Dubreuilh, X. H., and Raffin, M., "Experimental Density Flowfields over a Delta Wing Located in Rarefied Hypersonic Flows," Workshop on Hypersonic Flows for Reentry Problems, Antibes, France, Jan. 1990.

[9]Allegre, J., Dubreuilh, X. H., and Raffin, M., "Etude Experimental D'une Aile Delta Placee Dans Un Ecoulement Hypersonique Rarefie," Final Rept., Document SESSIA 340/88.802, Nov. 1988.

[10]Rault, D. F. G., "Aerodynamic Performance of Delta Wings in the Hypersonic Rarefied Flow Regime—Comparison of 3D DSMC Simulation with Wind Tunnel Data," Workshop on the Hypersonic Flows for Reentry Problems, Pt. II, Antibes, France, Jan. 1991.

[11]Legge, H., "Force and Heat Transfer Measurements on a Disc at 45°–90° Angle of Attack in Free Jet Flow Using Ar, He, N_2, H_2 as Test Gases," DFVLR-AVE Rept. IB 222-89, April 1989.

[12]Bird, G. A., *Molecular Gas Dynamics,* Clarendon, Oxford, England, UK, 1976.

[13]Bird, G. A., "Monte-Carlo Simulation in an Engineering Context," *Rarefied Gas Dynamics,* edited by S. S. Fisher, Vol. 74, Pt. I, Progress in Astronautics and Aeronautics, AIAA, New York, 1981, pp. 239–255.

[14]Bird, G. A., "Direct Simulation of Gas Flows at the Molecular Level," *Communications in Applied Numerical Methods,* Vol. 4, 1988, pp. 165–172.

[15]Blanchard, R. C., "Rarefied Flow Lift-to-Drag Measurements of the Shuttle Orbiter," International Council of the Aeronautical Sciences, Paper 86.2.10.2, Sept. 1986.